Eur. Phys. J. D **19**, 31–44 (2002)
DOI: 10.1140/epjd/e20020052

THE EUROPEAN PHYSICAL JOURNAL D
EDP Sciences

Widely usable interpolation formulae for hyperfine splittings in the $^{127}I_2$ spectrum

B. Bodermann[a], H. Knöckel, and E. Tiemann[b]

Institut für Quantenoptik, Universität Hannover, Welfengarten 1, 30167 Hannover, Germany

Received 17 July 2001 and Received in final form 17 October 2001

Abstract. Based on new systematic high precision measurements of hyperfine splittings in different rovibrational bands of $^{127}I_2$ in the near infrared spectral range between 778 nm and 816 nm, and the data in the range from 660 nm to 514 nm available from literature, the quantum number dependence of the different hyperfine interaction parameters was reinvestigated. As detailed as possible parameters were re-fitted from the reported hyperfine splittings in literature, considering that the interaction parameters should vary smoothly with the vibrational and rotational quantum numbers, and follow appropriate physical models. This type of consistency has not been sufficiently taken into account by other authors. To our knowledge it is now possible for the first time to separate the hfs contributions of the two electronic states $B^3\Pi_{0_u^+}$ and $X^1\Sigma_g^+$ for optical transitions in a very large wavelength range. New interpolation formulae could be derived for both states, describing the quantum number dependences of the nuclear electric quadrupole, of the nuclear spin-rotation and also of the nuclear spin-spin interactions. Using these new interpolation formulae the hyperfine splittings for the components with the quantum number condition $F - J = 0$ can be calculated with an uncertainty of $\leq$30 kHz for transitions in the wavelength range between 514 nm and 820 nm.

PACS. 33.15.Pw Fine and hyperfine structure – 33.20.Kf Visible spectra

1 Introduction

The iodine spectrum has shown to be a suitable frequency reference for laser frequency stabilisation from the visible to the IR spectral region (see references in [1], or *e.g.* [2–11]). Because of its rich spectrum and since it is easy to handle using a simple glass cell, iodine has also often been applied as a wavelength reference in the visible. Six of the wavelength standards recommended by the *Comité International des Poids et Mesures* (CIPM) for the realization of the meter [1] are lasers whose frequency is stabilised to iodine hyperfine components.

Additionally, the internal systematics of the rotational and vibrational structure of the molecular spectrum offers the possibility of predicting frequencies of a large number of transitions using known molecular parameters [12,13]. It has been shown that, at least for a limited spectral range and by analysing high precision frequency measurements on Doppler-free iodine lines, the interpolation of transition frequencies can reach a level of accuracy of few 10^{-9} or better [14,15]. To achieve such a level of prediction accuracy for Doppler-free iodine lines a detailed study of the hyperfine structure is necessary, besides a systematic determination of the rovibronic molecular structure. Numerous experimental and theoretical studies on the hyperfine structure of molecular iodine have been performed over the last 30 years [16–37]. Several authors have derived empirical prediction formulae that describe the dependences of the hyperfine structure on the vibrational and rotational quantum numbers. The most accurate of these empirical formulae up to now are limited to the visible spectral range [24].

We performed systematic experimental studies both on the rovibronic and on the hyperfine structure of $^{127}I_2$ in the NIR. Combining these measurements with data available from literature we were able to separate the contributions of the two electronic states and to derive new and improved formulae, which allow for an accurate prediction of transition frequencies of iodine lines both for the visible and the NIR spectral range. While the results concerning the rovibronic structure will be presented in connection with a precise potential determination in a forthcoming paper, here we present our results on the hyperfine structure.

After a short introduction to the physical background of the quantum number dependence of the hyperfine interactions the paper presents our own systematic measurements of the hyperfine structure of iodine lines in the

[a] *Present address:* Physikalisch-Technische Bundesanstalt, Bundesallee 100, 38116 Braunschweig, Germany.
[b] e-mail: tiemann@iqo.uni-hannover.de

near infrared. Then the data from the literature are revised, and interpolation formulae are derived for the relevant interactions. Finally, the accuracy of predictions of hyperfine splittings from these formulae is discussed.

2 Quantum number dependence of hyperfine interaction parameters

The hyperfine structure of the iodine molecule is usually described by an effective Hamiltonian [16]:

$$H_{\mathrm{hfs,eff}} = H_{\mathrm{eqQ}} + H_{\mathrm{SR}} + H_{\mathrm{SS}} + H_{\mathrm{TS}} \tag{1}$$

where H_{eqQ}, H_{SR}, H_{SS} and H_{TS} represent the (effective) nuclear electric quadrupole, the nuclear spin-rotation, the scalar nuclear spin-spin and the tensorial spin-spin interactions. The matrix elements of these terms can be separated into a product of different geometrical factors g_i and hyperfine parameters, *i.e.* eqQ, C, δ and d, respectively:

$$\langle (J'I'), F|H_{\mathrm{hfs,eff}}|(JI), F\rangle = eqQg_{\mathrm{eqQ}} + Cg_{\mathrm{SR}} + \delta g_{\mathrm{SS}} + dg_{\mathrm{TS}}. \tag{2}$$

The g_i are functions of appropriate angular momentum quantum numbers, named conventionally J, I and F, of the system and can be calculated with spherical tensor algebra. Expressions for these functions can be found in Tables Va and Vb of [16] or in [18]. The hyperfine parameters usually have to be determined experimentally for the hyperfine structure of each rovibrational transition. If these constants are derivable from extrapolation or interpolation for a specific rovibrational level, the hyperfine splitting can be calculated. The functional forms of these effective hyperfine parameters were explicitly derived by Broyer *et al.* [16] using a perturbation calculation up to second order. For both the ground state $X^1\Sigma_g^+$ and the exited state $B^3\Pi_{0_u^+}$ of the iodine molecule, that are $\Omega = 0$ states, these parameters $\chi(v, J)$ have the following structure for a level (v, J) of an electronic state:

$$\chi(v, J) = \chi_1(v, J) + \sum_p \frac{\chi_{2p}}{\Delta E^J_{v,v_p}} \langle v|v_p\rangle \cdot \tag{3}$$

Here χ_1 is the first order contribution of the discussed electronic state (B or X) and χ_{2p} are the second order contributions from the perturbing state p with energy difference $\Delta E_{v,v_p}$ between the levels (v, J) and (v_p, J) and the overlap integral $\langle v|v_p\rangle$ of the two vibrational states. This form is a simple approximation where the electronic matrix element will have only a weak dependence on the nuclear separation. χ_1 is an expectation value of the generally R-dependent interaction for the specific rovibrational state (v, J). Thus this part will be represented in the conventional form of a Dunham series in v and J,

$$\chi_1(v, J) = \sum_{l,k} \chi_1^{lk}(v + 1/2)^l [J(J + 1)]^k \tag{4}$$

where typically few members of this series are sufficient for describing a large set of experimental data. The coefficients χ_1^{lk} might be related to the potential of the electronic state, and thus a power expansion of χ with the internuclear distance R can be derived. This kind of analysis is performed by Spirko and Blabla [20] for the quadrupole coupling constant eqQ of I_2. For the present purpose we do not pursue this approach because no improved interpolation formulae are expected.

The sum over the perturbing states contains two different categories: the first one, where the electronic state is close by, so that the energy denominator plays an important role in the functional form of the parameter, and the second one, where the perturbing state is so far away that the whole contribution does not vary significantly with v_p. Then this latter part cannot be distinguished from the functional form of $\chi_1(v, J)$. Similar considerations were already successfully applied by Vigué *et al.* [17] for *ab initio* calculations of C_B for higher vibrational states v'. In iodine the states mainly perturbing the $X^1\Sigma_g^+$ have the same atomic asymptotes as X and are very weakly bound. Thus the energy denominator can be approximated by $\Delta E^J_{v,vp} \approx E_{v,J} - \overline{E}_p(3/2, 3/2)$, where $\overline{E}_p$ is an average of the perturbing levels and will have a value close to that of the atomic asymptote $^2\mathrm{P}_{3/2} + {}^2\mathrm{P}_{3/2}$ of iodine. Under these conditions the overlap integral $\langle v|v_p\rangle$ will not vary strongly with v_p, because the part of the wavefunction for small nuclear separation will almost stay constant while varying v_p up to the dissociation limit. Thus $\chi_{2p}\langle v|v_p\rangle$ can also be approximated by a simple and short power expansion in v and J.

Similarly, we can also approximate the functional form of the hyperfine parameters of the B state, only the dissociation asymptote is shifted to $^2\mathrm{P}_{1/2} + {}^2\mathrm{P}_{3/2}$ of iodine, and we introduce as an average energy for the perturbing state $\overline{E}_p(1/2, 3/2)$. In total, we will apply

$$\chi(v, J) = \sum_{lk} \chi_1^{lk}(v + 1/2)^l [J(J + 1)]^k + \frac{\sum_{lk} \chi_2^{lk}(v + 1/2)^l [J(J + 1)]^k}{E_v - \overline{E}}, \tag{5}$$

and $\overline{E}$ stands for $\overline{E}_p(3/2, 3/2)$ or $\overline{E}_p(1/2, 3/2)$.

From the derivation [16] of the second order contributions of the scalar and tensorial spin-spin interactions, *i.e.* the parameters δ and d, one sees that both are in close relation, but which depends on the electronic quantum numbers of the perturbing states, where we have to consider $\Omega_p = 0$ and 1. In the former case both differ in sign, in the latter case by a factor of two. Thus we can use the following formulae for the two interaction parameters

$$\delta = \delta_1(v, J) + \frac{\delta_2^0(v, J)}{E_{v,J} - \overline{E}} + \frac{\delta_2^1(v, J)}{E_{v,J} - \overline{E}} \tag{6}$$

$$d = d_1(v, J) - \frac{\delta_2^0(v, J)}{E_{v,J} - \overline{E}} + (1/2)\frac{\delta_2^1(v, J)}{E_{v,J} - \overline{E}}, \tag{7}$$

where the second term in each equation describes the perturbation due to $\Omega = 0$ states and the third term due to $\Omega = 1$ states.

Finally, it should be mentioned that by measuring optical transitions between X and B state usually (for $J \geq 10$) only differences between the hyperfine parameters can be determined, because the corresponding parameters of the two states are strongly correlated, if inferred from transitions with selection rules $\Delta F = \Delta J$, which is the case for most of the existing data; fitting spectra one obtains

$$\begin{aligned} \Delta eqQ &= eqQ_B - eqQ_X \\ \Delta C &= C_B - C_X \\ \Delta\delta &= \delta_B - \delta_X \\ \Delta d &= d_B - d_X. \end{aligned} \tag{8}$$

3 Measurements in the NIR and fitting procedure

We measured the hyperfine structure of 45 rovibrational transitions in the wavelength range between 778 nm and 816 nm. The experimental setup of Doppler-free saturation spectroscopy and the methods for analysing the hyperfine structure are described in detail in [8,27]. The hyperfine energies were derived from the diagonalization of a matrix which covers the rotational space J and $J\pm2$. The fits of the hyperfine structure include a line shape analysis of the measured lines, which permits calculation and correction of the frequency pulling or pushing due to overlapping profiles of neighbouring hyperfine components. The data and analysis of the (0–15) band (14 rotational lines) was already published in [27]. Typical spectral structures of the hyperfine interaction in iodine are published in many papers, *e.g.* in [27]. Thus we omit them here. With the exception of the transition P(1) $(v'-v'') = (0\text{–}14)$ (see below) from the 31 new measurements only differences of the hyperfine parameter according to equations (8) can be derived, because $J'' > 16$. For this reason, the ground state parameters eqQ_X, C_X, δ_X and d_X were set to plausible values (see below) and kept fixed, but the B state parameters eqQ_B, C_B, δ_B and d_B were fitted. In this way small influences of the separated parameters of X and B (because the parameters of the states are not correlated to 100%) could be included with sufficient accuracy and from the fit results and the fixed constants the true differences ΔeqQ, ΔC, $\Delta\delta$ and Δd were calculated.

For some transitions only few hyperfine components have been measured for experimental reasons, so that a determination of all four parameters was not possible. In these cases only eqQ_B and/or C_B have been fitted and the other parameters were set to fixed values, which were obtained in an iterative process from the fit of all measured bands and by application of the interpolation formulae at each iteration step.

The frequency of a specific hyperfine component depends differently on the individual hyperfine parameters. As an example, the energy splitting of the $F - J = 0$ (where F is the total angular momentum including nuclear spin) components is nearly independent of the C parameter. Therefore, it depends on the kind of the measured hyperfine components and on the quantum numbers of these components, whether a hyperfine parameter can reliably be derived from the measurement or not. As an example, for the R(138) 1–14 transition, where only the $F - J = 0$ components a_1, a_{10} and a_{15} (the hyperfine components are numbered from 1 to 15 for even J'' and from 1 to 21 for odd J'' in increasing order of energy) have been measured, only eqQ_B was determined. For the R(139) 1–14 line in contrast the components a_{12}, a_{13} and a_{14} were measured, whose hyperfine splitting is more suited for a determination of C_B. The measured lines, which have generally high vibrational levels for X ($v'' = 12$ to 17) and low for B ($v' = 0$ to 3), are listed in Table 1.

4 Determination of hyperfine parameters

The derivation of the hyperfine parameters consists of several iterations, which will be explained in detail to show the consistency of this approach. The first step aims to split off the weakest contributions, *i.e.* the spin-spin interaction by δ and d, for which only low accuracy can be expected and their influence on the other parameters will be negligible.

For the 0–15 band in earlier investigations no significant rotational dependence of the spin-spin parameters δ and d was inferred [27]. For five transitions of the 0–14 band and for the transitions R(180) 0–16 and R(188) 0–13 these parameters were obtained with significance. Because we consider transitions with ground state vibrational levels v'', of which the energetic distance to possible perturbing states is larger than 8 000 cm^{-1}, we expect the variation of δ_X and d_X with v'' to be negligible. So the variation of $\Delta\delta$ and Δd is attributed to their dependence on v'. The variations with J' of $\Delta\delta$ and Δd of the newly measured transitions sharing the common upper vibrational level $v' = 0$ and of the 0–15 band were examined thoroughly. While for Δd no significant dependence on J' can be detected, for $\Delta\delta$ the values for very high J' ($J > 180$) seem to decrease (see Tab. 1). But considering the relatively large uncertainties of these values, the interrelation between δ and d, and the missing tendency for Δd we believe this decrease to be of no significance. Thus we calculate weighted averages and find:

$$\Delta\delta = 10.3(30)\ \text{kHz}, \qquad \Delta d = -4.3(5)\ \text{kHz}. \tag{9}$$

These results are in very good agreement with our earlier results of the 0–15 band alone, where we found $\Delta\delta = 10.4(5)$ kHz and $\Delta d = -4.4(6)$ kHz [27]. New fits were run with these parameters fixed to the averages, varying only eqQ_B and C_B. The results for all lines in the near infrared are listed in Table 1. It shows in the fourth and fifth column the number of measured hyperfine components and the obtained standard deviation of the fits. The latter was always close to the experimental measurement error.

These results will be used to separate the contributions of the two electronic states by their different quantum number functions in v'', J'' and v', J', respectively. Figure 1 shows all derived ΔC as a function of $J(J+1)$. First, one recognizes that all results for $v' = 0$ concentrate

Table 1. Hyperfine parameters derived from measurements of iodine lines in the near infrared. The numbers of decimal places given are due to usage in the fit.

transition	ΔeqQ [MHz]	ΔC [kHz]	no. of comp.	std. dev. [kHz]
R(240) 0–12	1 960.696(32)	19.972(10)	11	26.5
P(164) 0–13	1 961.492(50)	19.084[1]	3	2.5
R(188) 0–13	1 961.021(27)	19.241(13)	15[2]	19.7
P(1) 0–14	−2 450.45(11)[4]	18.158[1]	9[4]	21.6
R(16) 0–14	1 961.880(43)	18.158[1]	5	17.9
R(18) 0–14	1 961.859(47)	18.158[1]	6	18.3
P(31) 0–14	1 961.554(501)	18.096(327)	4	35
R(56) 0–14	1 961.695(62)	18.364(91)	9	42
P(70) 0–14	1 961.664(17)	18.343(27)	7	11.1
R(78) 0–14	1 961.556(6)	18.401(25)	11	3.2
P(87) 0–14	1 961.548(16)	18.407(8)	17	6.6
R(96) 0–14	1 961.429(15)	18.487(16)	7	5.4
P(166) 0–14	1 960.580(90)	19.059[1]	2	-
R(174) 0–14	1 960.385(42)	19.028(11)	15	23.4
R(205) 0–14	1 959.672(25)	19.354(5)	19	21.8
R(138) 1–14	1 958.905(50)	19.661[3]	3	6.7
R(139) 1–14	1 958.905[3]	19.661(9)	3	7.2
P(148) 1–14	1 958.884(28)	19.709(53)	7	10.9
P(228) 1–14	1 957.233(152)	20.599(39)	5	14.3
R(0) 0–15	−489.290(580)[5]	18.125[1]	6	229.7
P(1) 0–15	−2 449.7(4)[4]	18.125[1]	7	48.3
P(7) 0–15	1 960.590(100)	18.128[1]	18	96.5
R(8) 0–15	1 960.920(120)	18.128[1]	13	71.2
R(9) 0–15	1 960.950(130)	18.128[1]	17	134.8
R(10) 0–15	1 960.760(100)	18.129[1]	13	55.5
R(16) 0–15	1 960.760(60)	18.134[1]	12	38.4
R(19) 0–15	1 961.151(137)	18.138[1]	2	-
R(39) 0–15	1 960.860(20)	18.218(29)	21	23.4
P(61) 0–15	1 960.780(30)	18.236(21)	19	19.2
P(79) 0–15	1 960.750(20)	18.327(12)	21	20.4
R(92) 0–15	1 960.550(30)	18.404(14)	11	5
P(94) 0–15	1 960.510(30)	18.384(10)	11	5
R(96) 0–15	1 960.537(49)	18.419(25)	11	7.2
R(99) 0–15	1 960.450(20)	18.418(12)	18	15.6
P(104) 0–15	1 960.517(13)	18.433(5)	9	2.3
P(105) 0–15	1 960.475(10)	18.422(9)	6	2
R(113) 0–15	1 960.315(18)	18.532(12)	5	10.4
P(239) 0–15	1 957.511(43)	19.745(37)	9	33.7
R(117) 2–15	1 956.465(149)	20.282(46)	14	25
P(172) 0–16	1 958.206(148)	19.029[1]	2	-
R(180) 0–16	1 958.028(25)	18.972(13)	9	18.3
P(43) 3–16	1 954.287(53)	20.459(59)	21[2]	18.9
P(34) 0–17	1 958.986(63)	18.063[1]	3	4
R(42) 0–17	1 958.831(57)	18.085(98)	11	18.4
R(44) 0–17	1 958.900(115)	18.094[1]	2	-

[1]Not fitted, averaged values from equations (10–13) for ΔC, $\Delta\delta$ and Δd, [2]hyperfine pattern partly overlapped by other lines, [3]combined analysis of R(139) and R(138) because of specific hyperfine components, [4]eqQ_X separately, [5]eqQ_B separately.

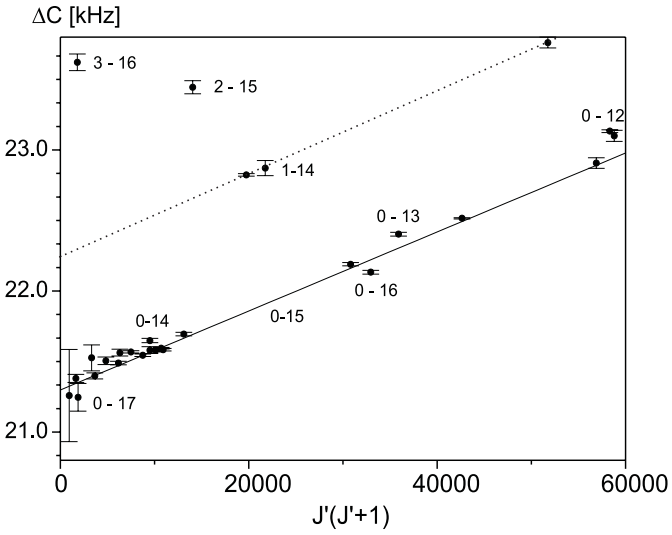

Fig. 1. Rotational dependence of ΔC. Solid line belongs to $v' = 0$ bands.

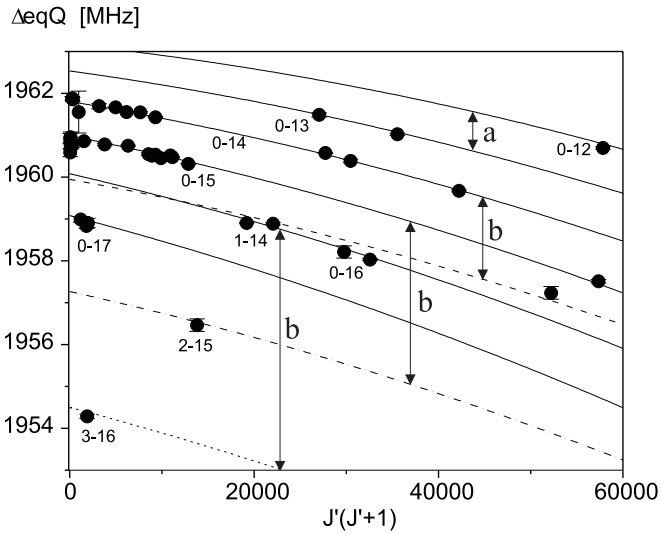

Fig. 2. Measured ΔeqQ of near infrared lines as function of the rotational energy. Solid lines belong to $v' = 0$ bands, vertical arrows: "a" marks variation in v'', "b" variation in v'.

around one single line, and the few other measurement points can be ordered by parallel shifting this line to the groups for $v' = 1$, $v' = 2$, and $v' = 3$ (example dotted line for $v' = 1$). Thus this diagram clearly directs us, that the main variation of ΔC with quantum numbers is related to the dependence on the excited state. Only the large set of data for $v' = 0$ and several different v'' (from 12 to 17) indicates a trend that C_X increases slightly with increasing v''.

This characteristic behaviour is qualitatively as expected, because the vibrational levels of the B state are much closer to perturbing levels of $\Omega = 1$ than those of the X state. These observations will be embedded in the overall analysis of the variation of ΔC and separately of C_X and C_B in Section 6.1.

Figure 2 shows an overview of ΔeqQ as a function of the rotational energy, together with curves derived from first fits to equations (14, 15) to guide the eyes. As stated above for high rotational quantum numbers ($J > 10$) it is very difficult to derive separate hyperfine parameters of the electronic states from optical transitions. But differences in trends due to quantum numbers can already be observed. In Figure 2 we can read off the order of variation in the ground state when we take the separation of the line for the band (0–12) and for band (0–13), which is roughly -1 MHz (arrow a), consistent also with the observations from the P(1) lines (see below). For the excited state we obtain from the line separation between band (0–14) and (1−14) − 2 MHz and similarly for the large separation of the other bands, indicated by arrows b. Thus, eqQ of the X state increases with increasing vibrational quantum number, but it decreases in the case of the B state.

For transitions P(1), however, we have $J' = 0$ and therefore the hyperfine structure of these transitions is nearly completely determined by the hyperfine parameters of the ground state. (An analogous statement is true for transitions R(0), where the hyperfine structure is nearly completely determined by the hyperfine parameters of the B state.) Unfortunately, due to the small thermal population of states with such low J'' the signal-to-noise ratio for these transitions usually is very low. This is even more severe for NIR transitions, where the cells have to be heated to several 100 °C, than for transitions in the visible. Nevertheless, in [27] we already presented a measurement of the P(1) 0–15, which allowed us to determine a value of $-2\,449.7(4)$ MHz for $eqQ_X(v'' = 15)$. Now we were successful in measuring the P(1) 0–14 transition with even an improved signal-to-noise ratio. Despite this improvement of the S/N, a determination of C_X, δ_X and d_X for this transition is still not possible, because the contributions by these magnetic interactions are very small for low J levels. Additionally, from the 9 measured hyperfine components of our present measurement only 4 can be attributed to not blended lines. We obtain a value of $eqQ_X = -2\,450.45(11)$ MHz, which gives an independent measure of the variation of the quadrupüole interaction in the ground state.

5 Analysis of all data available on $^{127}I_2$ from literature

The data available in literature were revised, and some inconsistencies were found, which lead to unphysical variations of the hyperfine parameters from one level to another. The reason seems to be the evaluation methods applied by the different authors.

We decided to re-analyse the whole available data using our methods in order to obtain highly consistent values for the hyperfine parameters. In some cases only the fitted hyperfine parameters were published, so that a new analysis was not possible. In these cases we used the published values [30,31,37].

Table 2. Hyperfine parameters for the X state from literature.

level v'', J''	eqQ_X [MHz]	C_X [kHz]	δ_X [kHz]	d_X [kHz]	source
83, 13	−1 554.6(5)	62.6(50)	0[1]	0[1]	[30]
81, 13	−1 629(3)	-	-	-	[33]
79, 13	−1 692(1)	-	-	-	[33]
76, 13	−1 781(2)	28(4)	0[1]	0[1]	[31]
62, 13	−2 128(1)	-	-	-	[33]
11, 13	−2 455(2)	7.9(10)	0[1]	0[1]	[32]
1, 0–10	−2 459.9(32)	0[1]	0[1]	0[1]	[37]
0, 0–6	−2 451.3(35)	0[1]	0[1]	0[1]	[29]
0, 15	−2 452.59699(45)	3.1543(29)	3.701(23)	1.519(18)	[26]
0, 13	−2 452.58514(45)	3.1536(33)	3.708(22)	1.528(18)	[26]
	−2 452.5837(16)	3.162(8)	3.66(3)	1.58(5)	[25]
0, 54	−2 453.088(24)	2.904(40)	3.705	1.524	[4]
0, 56	−2 453.132(11)	3.306(21)	3.705	1.524	[4]

[1]Values fixed to zero during their fit by corresponding authors.

Table 3. Hyperfine parameters for the B state, mainly from literature.

level v', J'	eqQ_B [MHz]	C_B [kHz]	δ_B [kHz]	d_B [kHz]	source
62, 27	−569.132(35)	938.739(78)	565.98(226)	−410.71(205)	[2]
43, 12	−558.617(3)	190.315(10)	0.30(3)	−99.9(1)	[2,19]
32, 58	−544.772(40)[1]	-	-	-	[4]
32, 57	−544.751(11)	89.656(21)	−6.943(86)	−42.701(78)	[4]
32, 53	−544.656(24)	89.004(41)	−7.04(12)	−42.54(11)	[4]
26, 13	−534.842(20)	62.099(62)	−5.56(83)	−27.14(74)	[1,41][2]
13, 0–10	−510.3(42)	32.5(6)	−30.2(23)	−9.9(16)	[37]
12, 0–6	−509.9(15)	49(11)	0[3]	0[3]	[29]

[1]From extrapolation in [4], [2]new fit from combined data of corresponding papers (std. dev. 5 kHz) X state values from [4] (R(13)), [3]values fixed to zero.

As far as hyperfine splittings of a transition had been measured by more than one author, we used weighted averages of their frequencies for our fits.

The fitting procedure for the hyperfine structure is already described above and in detail in [8,27]. For a calculation and correction of the frequency pulling or pushing due to overlapping profiles of neighbouring hyperfine components we used the experimental lineshapes of the hyperfine lines. In cases, where line profile data were not published, we estimated these parameters from the linewidth of the laser emission, iodine pressure, predissociation rate, and from the kind of modulation technique used for detection. To our knowledge, the data of Gill *et al.* [28] for the transitions R(98) 43–2 and 27–3 were never analysed before. The reanalysis was done iteratively in several steps. Initially all data were fitted in the same way. For the ground state we used the values for $v'' = 0$, $J'' = 13$ obtained by Yokozeki *et al.* [25]: $eqQ_X = -2\,452.584$ MHz, $C_X = 3.162$ kHz, $\delta_X = 3.66$ kHz and $d_X = 1.58$ kHz. This choice is arbitrary, but doesn't make any problem as long as the fit is only sensitive to the differences between the parameters of both states (see discussion in Sect. 3). The values were kept fixed during the fits. For most of the data in this iteration all four parameters eqQ_B, C_B, δ_B and d_B were fitted, and from these and the above mentioned ground state values differences of hyperfine parameters were calculated as the final result. For those transitions, where the experimental errors of the measurements are relatively large, the spin-spin parameters turned out to be not significant. These transitions were re-analysed in a second step setting the parameters δ_B and d_B to the values obtained by the formulae derived below (Eqs. (12, 13)) and varying only C and eqQ. In other cases too few lines are known, so that even C was fixed using the formulae below and only eqQ was fitted.

For a reliable separation of the quantum number dependence of the hyperfine parameters of either electronic state the parameters of one of the states must be known as absolute values. An overview of such derived values for both states is listed in Tables 2 and 3. They were obtained either by measurements of transitions with low angular momentum J [2,19,24,27,29,37], or stimulated Raman two-photon transitions [26,30–32] or using a molecular beam Rabi-type setup [25], or measuring cross-over resonances in saturation spectroscopy [4].

For a long time the parameters obtained by Yokozeki and Muenter [25] for $v'' = 0$, $J'' = 13$ were mostly accepted for the ground state. Recently, Wallerand *et al.* [26]

Table 4. New evaluation of hyperfine parameters from published spectra. For P(84) 33–0 the fit was adopted from the original reference [3].

transition	ΔeqQ [MHz]	ΔC [kHz]	$\Delta\delta$ [kHz]	Δd [kHz]	source	std. dev. [kHz]
R(26) 62–0	1 883.453(10)	935.563(22)	562.51(63)	−412.56 (57)	[2]	18
R(98) 58–1	1 880.100(16)	829.136(8)	355.77(76)	−502.03(78)	[1]	29
R(15) 43–0	1 893.951(8)	187.368(26)	−3.05(40)	−102.04(46)	[1]	1.3
P(13) 43–0	1 893.968(4)	187.140(6)	−3.18(21)	−101.78(23)	[1]	0.59
R(98) 43–2	1 894.375(80)	208.743(63)	−2.61[1]	−102.5[2]	[28]	66
R(134) 36–0	1 902.209(18)	128.696(7)	−7.8(13)	−67.5(19)	[1]	4
R(122) 35–0	1 903.759(2)	116.101(1)	−9.45(13)	−60.29(12)	[4]	0.82
P(119) 35–0	1 903.888(3)	114.955(1)	−9.215(2)	−59.847(25)	[1]	1.2
R(106) 34–0	1 905.290(4)	104.829(2)	−9.88(25)	−54.08(23)	[1]	0.86
R(86) 33–0	1 906.838(4)	95.037(3)	−10.32(26)	−48.86(23)	[1]	0.81
P(84) 33–0	1 906.911(2)	94.582(2)	−10.51(13)	−48.59(12)	[3]	0.61 ([3])
P(83) 33–0	1 906.928(7)	94.485(4)	−10.17(43)	−49.40(52)	[1]	1.9
R(57) 32–0	1 908.380(2)	86.413(2)	−10.32(10)	−44.39(12)	[1]	0.61
R(56) 32–0	1 908.381(2)	86.347(2)	−10.64(13)	−44.24(12)	[4]	0.76
P(54) 32–0	1 908.433(2)	86.105(2)	−10.78(13)	−44.12(12)	[4]	0.47
P(53) 32–0	1 908.455(11)	86.026(13)	−10.71(91)	−44.46(99)	[1]	3.5
R(106) 28–0	1 914.429(16)	70.267(8)	−8.0(11)	−34.6(10)	[1]	3.7
P(133) 27–3	1 917.04(81)	68.081(73)	−6.4[1]	−33.4[2]	[28]	104
R(12) 26–0	1 917.731(40)	58.908(81)	−8.7(20)	−28.9(19)	[1]	5
P(62) 17–1	1 933.335(47)	37.379(35)	−1.1(4)	−19.7(17)	[1]	62
R(34) 17–6	1 934.073(21)	37.02(63)	−0.2(35)	−14.2(15)	[19]	16
R(48) 15–5	1 937.532(61)	33.471(99)	−2.5[1]	−16.80[2]	[1]	29
P(62) 11–2	1 944.71(70)	28.19[4]	−10.33[1]	−18.09[2]	[40]	820
P(48) 11–3	1 944.639(52)	27.505(40)	−12.3(25)	−20.34(91)	[1]	1.7
R(127) 11–5	1 944.656(15)	28.389(5)	−15.19(30)	−20.74(33)	[1]	8.5
R(161) 9–0	1 947.95(23)	26.987(50)	−16.5[1]	−19.8[2]	[40]	271
R(47) 9–2	1 948.006(20)	25.153(6)	−15.60(26)	−19.70(34)	[1]	2.3
R(16) 8–5	1 950.110(71)	22.771[3]	−14.9[1]	−18.4[2]	[1]	17
P(10) 8–5	1 950.62(27)	24.766	−14.9[1]	−18.4[2]	[1]	103
R(39) 7–4	1 951.883(92)	23.319(84)	−12.1(4.1)	−16.3(63)	[7]	63
P(33) 6–3	1 953.698(10)	22.606(30)	−6.67(67)	−13.42(83)	[1,9–11]	4.6
P(84) 5–5	1 955.9(13)	22.0(15)	−2.1[1]	−10.6[2]	[21]	519
R(69) 3–4	1 960.53(99)	21.6(11)	5.8[1]	−6.0[2]	[21]	612

[1] $\Delta\delta$ from equation (12), fixed in fit of hyperfine structure, [2] Δd from equation (13), fixed in fit of hyperfine structure, [3] ΔC from equations (10, 11) and fixed in the fit of the hyperfine structure.

succeded in measuring the same levels with improved accuracy, using a Raman setup, and confirmed the values by [25] within the limits of the earlier uncertainty. Recent results from [4] fix the parameters for $v'' = 0$, $J'' = 54$ and 56, and the rotational dependence of eqQ_X could be well established for $v'' = 0$.

Since the transitions $v' = 43$, $J' = 12 - v'' = (11, 62, 76, 79, 81, 83)$, $J'' = 13$ were measured [30–33], with the common level $v' = 43$, $J' = 12$ known from [1,2], the eqQ_X parameter for these levels could be derived. But the values for eqQ_X published by Koffend *et al.* [30,33] refer to an older determination of $eqQ_X(v'' = 0,\ J'' = 13)$ [34]. So we corrected these values using the results of Yokozeki *et al.* [25]. Unfortunately, for the measurements by Hackel *et al.* [32] the reference was not reported, so that a correction of this value is not possible, and this value was not used in deriving the interpolation formulae.

Also the extensive data sets obtained by Pique *et al.* [18,35] and by Bacis *et al.* [36] on the exited vibrational levels of the X ($v'' \geq 26$) and of the B state ($v'' \geq 61$) were considered. These data are very useful for an identification of the distortions due to hyperfine mixing with other electronic states, since these distortions increase rapidly, when approaching the dissociation limit of the considered state. But they were not included in the fits and therefore are not mentioned in the tables.

The results of our fits of parameter differences are shown in Table 4. The transitions, where extrapolated values for parameters have been used, are clearly marked. In most cases the fits are of improved or equal quality as compared to the report in the corresponding paper.

The improvements are probably a result of the corrections of frequency pulling or pushing due to overlapping lines. For a consistent fit of the transition R(161) 9–0 [40] we omitted the measured value for the hyperfine component a_7. The deviation between the calculated value from the new fit and the measured one for a_7 is very close to exactly 1 MHz, thus indicating a possible typing error. Only for the transitions R(134) 34–0 and R(48) 15–5 the standard deviations of the fits are slightly larger than the results collected in [23].

6 Evaluation of the quantum number dependence of the hyperfine parameters and new interpolation formulae

In the formulae derived in this section for the different hyperfine interactions the individual parameter values are given without uncertainties, because of significant correlations between the parameters. The number of decimal places given is chosen for precise reproduction of the hyperfine parameters. The limits of uncertainty for the effective hyperfine interactions are discussed in Section 7.

6.1 Quantum number dependence of C_X and C_B

For the nuclear spin-rotation parameters C_X and C_B we expect a hyperbolic dependence on the vibrational energy $E(v)$ of X or B due to the perturbing states sharing the same asymptote as the state considered, according to equation (5).

The values for C_X presently known are listed in the third column of Table 2. There are determinations for the highly exited vibrational levels $v'' = 76$ [31] and $v'' = 83$ [30]. For $v'' = 11$ there is a value from [32], but the most precise ones exist for $v'' = 0$. We already explained above, that from our measurements in the near infrared C_X was found to vary slightly for low v'' in the interval $(12 \leq v'' \leq 17)$, but a derivation of independent values for C_X was not directly possible, because of the high J measured.

The values of C_X of $v'' = 0$, 76 and 83 were taken together with differences of ΔC with common B level from the NIR data, and the model of equation (5) was applied in a nonlinear fit. The value of $v'' = 11$ [32] always deviated strongly in preliminary fits, so it was omitted in the final runs. Also there seems to be a problem with the two values C_X for $J'' = 54$ and $J'' = 56$ in $v'' = 0$, which differ by more than 10% from each other, without any obvious physical reason. Recent results by Bordé yield a constant C_X for $v'' = 0$ [42]. Thus, data of [4] were not included in the fit.

The fit was iterated, first taking the absolute values for the ground state from Table 2, then adding those NIR data with common $v' = 0$ (assuming linear dependence of C_B for $v' = 0$ in $J'(J'+1)$, which is confirmed below) in order to determine the parameters for the ground state first. It turns out that a linear term in the vibrational quantum number is sufficient to describe the whole series appropriately. The averaged energy $\overline{E}$ of perturbing levels was also varied. This gives a slightly better fit for the two values at high vibrational quantum numbers. Any rotational dependence is not significant in the data and was therefore omitted. As a result C_X is represented by:

$$C_X[\mathrm{kHz}] = 1.9245 + 0.01356(v'' + 1/2) - \frac{15\,098}{E(v'')[\mathrm{cm}^{-1}] - 12\,340}\,. \quad (10)$$

$E(v'')$ is the energy of the vibrational level (v'', $J'' = 0$), referred to the lowest vibrational level ($v'' = 0$, $J'' = 0$), $E(v'') = G_X(v'') - G_X(v'' = 0)$, which can be found tabulated in sufficient precision in [13]. According to this result we calculate for the vibrational levels $v'' = 12$ to $v'' = 17$ values from 3.63 kHz to 3.86 kHz, which can be used later on to derive separate values of C_B from the NIR data set.

Then the parameters for the ground state were fixed and all other data were included to fit the parameters C_B and ΔC for the excited state. Inspection of Table 4 shows a large variation of ΔC approaching the dissociation limit of the B state. For parity electronic reasons only a coupling with 1_u states contributes to the effective spin-rotation interaction in the B state. Two different 1_u states share the same dissociation limit ($^2\mathrm{P}_{1/2}$–$^2\mathrm{P}_{3/2}$) as the B state. It is known from the work by Pique *et al.* [18], that both 1_u states couple to the B state, and that in the vicinity of the dissociation limit significant contributions to C_B are due to these states. To avoid the complication with the two different perturbing states at the asymptote, for which detailed information is missing, we restricted the fit to the experimental data with $v' \leq 43$ or $E(v) \leq 19\,500\ \mathrm{cm}^{-1}$, to keep the distance to the perturbing states large enough, so that one effective interaction according to equation (5) is appropriate. In this manner we obtained:

$$\begin{aligned} C_B[\mathrm{kHz}] = {} & -4.016 - 0.1501(v' + 1/2) \\ & -(3.957 \times 10^{-4})J'(J'+1) \\ & -1.767 \times 10^{-5}(v' + 1/2)J'(J'+1) \\ & -\frac{110\,704 + 1.862J'(J'+1)}{E(v')[\mathrm{cm}^{-1}] - 19\,986}. \end{aligned} \quad (11)$$

$E(v')$ is the energy of the vibrational level (v', $J' = 0$), again referred to the lowest vibrational level ($v'' = 0$, $J'' = 0$), $E(v') = G_B(v') - G_X(v'' = 0)$ and is tabulated *e.g.* in [13]. To account for the strong increase of C_B in the range $v' > 43$ $\overline{E}$ was used as an effective parameter and adjusted by the fit. Finally, the parameters C_X and ΔC of the ground state were adjusted again while keeping those of the excited state fixed, and then the same for C_B and ΔC, until no further improvement was achieved. Equations (10, 11) already show the final result.

For a quantitative comparison with former approaches we calculated the values of C_B using the formulae proposed by Razet *et al.* [24] (formula (10b)) and by Arie *et al.* [22] (formula (3)). Figure 3 shows the differences between experimental values and the values calculated with

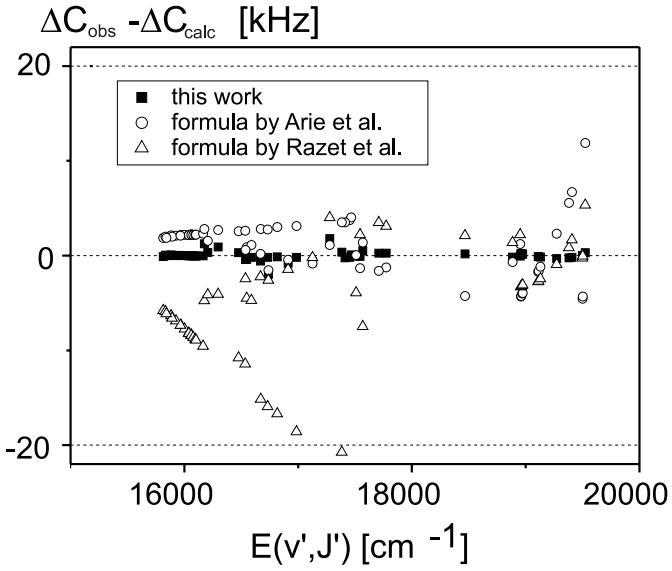

Fig. 3. Comparison of prediction formulae for ΔC.

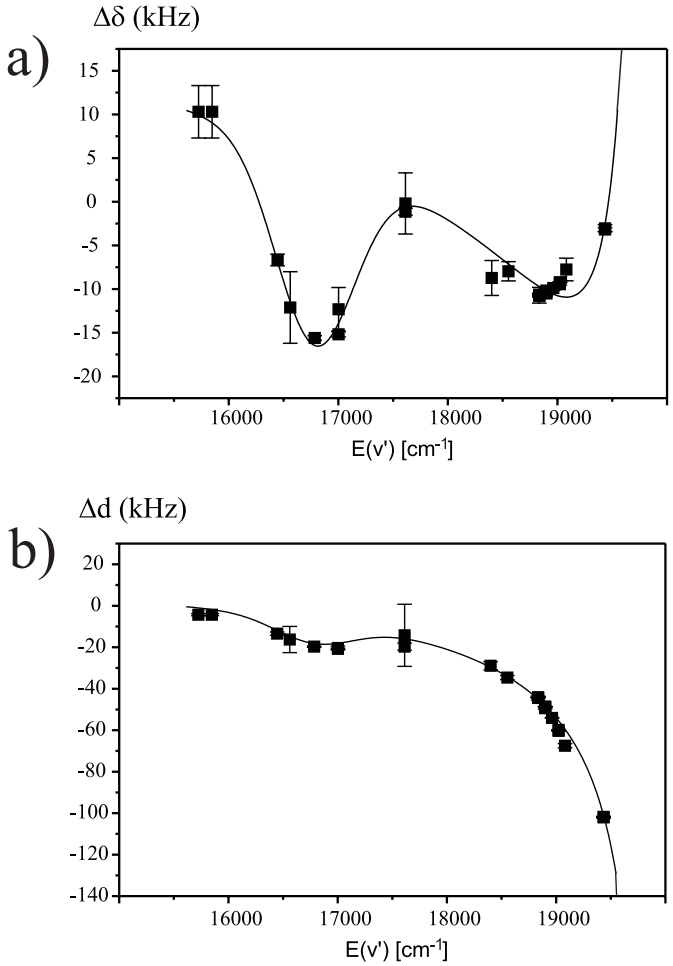

Fig. 4. (a) $\Delta\delta$ and (b) Δd as functions of $E(v')$, the vibrational energy in the excited state. Values for $v' = 58$ and 62 above 19 500 cm^{-1} are out of scale.

equations (10, 11) (squares), using the approach by Arie *et al.* (circles) and using the approach by Razet *et al.* (triangles). A satisfying description of the NIR data (between 16 000 cm^{-1} and 17 000 cm^{-1} in Figure 3 is only obtained by equations (10, 11). The values calculated by the approach of Arie *et al.* for these transitions are systematically about 3 kHz too small, and the deviation increases slightly for transitions with higher J'. The values obtained from the Razet formula are generally too big for the NIR transitions (triangles to lower part of Fig. 3); the deviations are about 6 kHz for small J', but increase rapidly with increasing J'. Obviously, the description of the rotational dependence of ΔC given by the Razet formula is inadequate for the NIR data. The description of the data with $v' > 2$ is also significantly improved using equations (10, 11). For the formulae by Arie *et al.* and Razet *et al.* an increase of the deviations is observed in the energy range around 19 500 cm^{-1}, corresponding to v' from 32 to 36 and higher J' (see Fig. 3), but these formulae describe the experimental values derived for $v' = 43$ [2]. All these deviations are much reduced using equations (10, 11). The maximum deviation between calculated and measured values is less than 2 kHz, the rms deviation is 0.5 kHz. The maximum deviation is more than 23 kHz for the formula by Razet *et al.* (out of scale in Fig. 3) and about 15 kHz for the formula by Arie *et al.*

6.2 Nuclear spin-spin interactions

From equations (6, 7) it is obvious, that the spin-spin interaction parameters are not independent of each other. Therefore, a common description of the quantum number dependence of these parameters is reasonable. Absolute values for the ground state parameters δ_X and d_X are known for the levels $v'' = 0$, $J'' = 13$ and $J'' = 15$ [25,26]. However, for the ground state levels of interest here ($v'' \leq 17$) the variations of these parameters are expected to be of comparable relative magnitude as the variation of C_X, which will be then within the experimental uncertainties for $\Delta\delta$ and Δd. So it is reasonable to assume constant values for the ground state and attribute all variations to the excited state. We took the averaged values for δ_X (3.705 kHz) and d_X (1.524 kHz) from [26] for $v'' = 0$, $J'' = 13$ for all levels $v'' \leq 17$. $\Delta\delta$ and Δd are shown in Figure 4 as functions of the energy in the excited state $E(v')$. The strong increase of these parameters approaching the dissociation limit is again due to the significant hyperfine mixing of the B state with electronic states sharing the same dissociation limit ($^2P_{3/2} + {}^2P_{1/2}$). According to the results of Pique *et al.* [18] four other states ($1'_g$, $1''_g$, 0^-_g, 0^-_u) couple to the B state, in addition to the two states $1'_u$ and $1''_u$ already mentioned. Since states with different symmetry (even-odd) contribute to the spin-spin interaction with opposite sign (see Sect. 2), these contributions partly compensate each other. Because of the different signs of δ_B and d_B for $E(v') > 19\,500$ cm^{-1} ($v' \leq 43$) the dominant contributions to the spin-spin interaction in the asymptotic range are due to an effective 0_g state. So one could try to describe this global tendency for these

parameters using equations (6, 7) with $\delta_2^1(v', J') = 0$. The values of δ_B vanish at $E(v') \approx 19\,500$ cm^{-1}, while $d_B(19\,500\ \text{cm}^{-1}) \approx 100$ kHz. This indicates, that for lower v' the influence due to 1_u states is important, leading to a compensation of δ_B at $E(v') \approx 19\,500$ cm^{-1}, and for d_B the contributions due to both the 1_u states and the 0_g^- states have negative sign, so that no compensation occurs.

Additionally, in the range $16\,000\ \text{cm}^{-1} \leq E(v') \leq 17\,700\ \text{cm}^{-1}$ a modulation for d_B and δ_B is visible, indicating a local perturbation due to a crossing state. From investigations on the predissociation of the B state a weak gyroscopic and magnetic dipole coupling between the B state and a 1_u state crossing the B state near level $v' = 5$ ($\approx$16 400 cm^{-1}) [38,39] is known.

This coupling induces a shift of the levels of the B state. A qualitative estimate of the level shift with the help of the observed Franck-Condon density in the predissociation analysis [38,39] compares quite well to the modulations observed in the curves for d_B and δ_B, indicating, that these modulations are caused by the weak magnetic dipole coupling of the 1_u and the B state.

However, for C_B such a modulation was not observed, which shows, that the gyroscopic coupling is much weaker than the magnetic dipole coupling between these two states. This result is consistent with the predissociation rates measured by Vigué *et al.* [38], which are about three orders of magnitude smaller for the gyroscopic predissociation than for the hyperfine predissociation.

For a highly precise description of d_B and δ_B a Gaussian function term was added to the equations (6, 7) characterizing the local maximum of the frequency shifts. This modification allows to simultaneously fit the data for d_B and δ_B for $E(v') < 19\,500$ cm^{-1}. We fitted the values given in Tables 3 and 4 both for δ, $\Delta\delta$ and for d and Δd. The results are:

$$\begin{aligned}\Delta\delta[\text{kHz}] = 31.57 &- \frac{32\,452}{E(v')[\text{cm}^{-1}] - 19\,896} \\ &+ \frac{126\,257}{E(v')[\text{cm}^{-1}] - 20\,687} \\ &- 22.41 \exp\left(-\frac{(E(v')[\text{cm}^{-1}] - 16\,787)^2}{260\,267}\right) \quad (12)\end{aligned}$$

$$\begin{aligned}\Delta d[\text{kHz}] = 19.56 &+ \frac{32\,452}{E(v')[\text{cm}^{-1}] - 19\,896} \\ &+ \frac{1}{2}\left\{\frac{126\,257}{E(v')[\text{cm}^{-1}] - 20\,687}\right. \\ &\left. - 22.41 \exp\left(-\frac{(E(v')[\text{cm}^{-1}] - 16\,787)^2}{260\,267}\right)\right\}. \quad (13)\end{aligned}$$

The standard deviation of the fit is 2 kHz. The resulting curves for Δd and $\Delta\delta$ are shown in Figure 4 as full lines. Equations (12, 13) represent the spin-spin parameters for $E(v') < 19\,500$ cm^{-1} ($v' \leq 43$). The B state parameters δ_B and d_B are obtained from equations (12, 13) by adding 3.705 kHz and 1.524 kHz, respectively.

For the intermediate range $43 < v' < 70$ a precise description of the spin-spin parameters is more difficult because a better knowledge of the different perturbing states and much more precise experimental data would be needed. For the asymptotic range $v' > 70$ Pique *et al.* [18] already investigated $d_B(E(v'))$ and $\delta_B(E(v'))$ in detail.

6.3 Nuclear electric quadrupole interaction

The above results for the magnetic hyperfine interactions permit an estimation of the contributions of the second order terms to the effective eqQ parameters according to the analyses of [16,18]. They are of the order of experimental accuracy for levels $v' \leq 43$ of the B state and even smaller for $v'' \leq 17$ of the X state. Thus such contributions will not influence the global quantum number dependence of the nuclear quadrupole coupling parameter in the above range.

For a description of the quantum number dependence of eqQ we fitted the experimental values for eqQ_B, eqQ_X and ΔeqQ using a power series according to equation (4) both for the B and the X state simultaneously. Good results were achieved using 11 fit parameters in total. For the vibrational dependences both of eqQ_B and eqQ_X three parameters were necessary. The rotational dependences of eqQ_B and eqQ_X are well described using three and two parameters, respectively. The fit is based on the measured values given in Table 1, the values from [4,25,26] of 2, and all values of Tables 3 and 4 with $v' \leq 43$, and it gives a 1σ standard deviation of 5 kHz.

The results for $eqQ_B(v', J')$ and $eqQ_X(v'', J'')$ are summarized in the following equations:

$$\begin{aligned}eqQ_X[\text{MHz}] = &-2\,452.2916 - 0.542(v'' + 1/2) \\ &+0.4534 \times 10^{-1}(v'' + 1/2)^2 \\ &-0.1927 \times 10^{-3} J''(J" + 1) \\ &+0.694 \times 10^{-5}(v'' + 1/2)J''(J'' + 1) \quad (14)\end{aligned}$$

$$\begin{aligned}eqQ_B[\text{MHz}] = &-487.879 - 1.8621(v' + 1/2) \\ &+0.12511 \times 10^{-3}(v' + 1/2)^3 \\ &-0.1281 \times 10^{-3} J'(J' + 1) \\ &-0.225 \times 10^{-5}(v' + 1/2)J'(J' + 1) \\ &-0.308 \times 10^{-9}[J'(J' + 1)]^2. \quad (15)\end{aligned}$$

The fit shows low correlations between the set of vibrational expansion parameters of the X state and that of the B state. Therefore, the functions for $eqQ_X(v'')$ and $eqQ_B(v')$ describe the vibrational dependences of these parameters quite independently. This is not necessarily true for the rotational dependences. Figure 5 shows the residuals of the fit. The agreement between measured and calculated values is mostly within the experimental errors. For few values the deviation obs-cal is somewhat greater than the corresponding uncertainty. Some are lines with low $J'' \leq 16$, and unrecognized lineshifts caused by weak cross-overs overlapping normal lines might be a reason for an underestimated uncertainty.

If formula (14) is reduced to $v'' = 0$, it is close to the formula given in [4] for the rotational dependence of eqQ_X for $v'' = 0$. A comparison of eqQ_X calculated from both

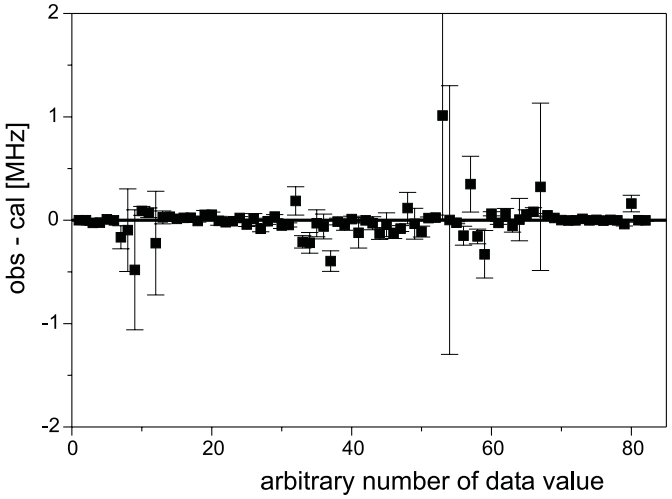

Fig. 5. Residuals of the fit of eqQ_X, eqQ_B and ΔeqQ to demonstrate the quality of the fit.

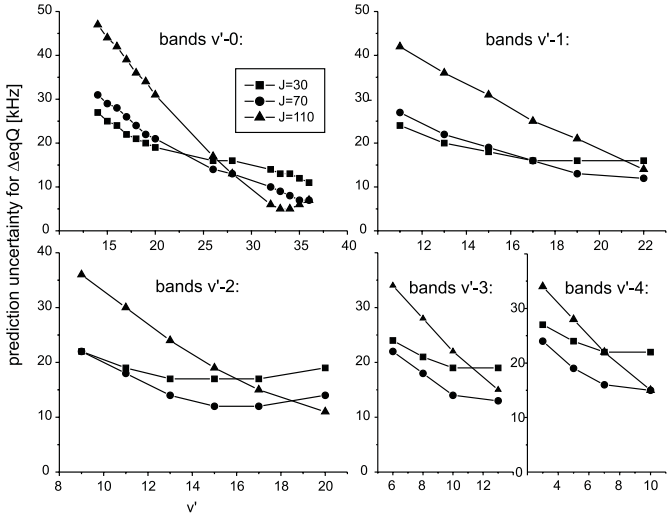

Fig. 6. Prediction uncertainties for ΔeqQ of selected bands and rotational quantum numbers.

formulae in the interval $0 < J'' < 60$ yields a maximum difference of 25 kHz, well within the present prediction uncertainty. But the present formula also describes the rotational dependence in the higher vibrational levels of the ground state quite accurately, the 2σ prediction uncertainty for eqQ_X is less than 50 kHz in the range from $v'' = 12$ to $v'' = 17$ for $J'' \leq 200$.

Calculating eqQ_X ($v'' = 11$, $J'' = 13$) from these formulae, however, we obtain a difference of 2.5 MHz to the experimental value, slightly above the reported uncertainty. The experimental value of $eqQ_X(v' = 11)$ (which was not included in the fit) by Hackel *et al.* [32] was derived from the measured transition P(13) 43–11, but, as already mentioned above, it is not clear to which value for eqQ_B ($v' = 43$, $J' = 12$) this result refers. So it might be shifted systematically due to a different parameter used for the upper state as compared to that used in this work.

Also the determination of eqQ_X by Wakasugi *et al.* [37] is about 7 MHz below the calculated value. The experimental value (also omitted from the fit) is derived from the measured hyperfine splitting of the band head of the 13–1 band ($J'' = 0$–10). The corresponding value for $eqQ_B(v' = 13)$, derived from the same measurements, also shows the greatest deviation from the calculated value. Due to the low signal-to-noise ratio and the strong overlapping transitions typically observed in band heads, and because of the large shift between their experimental value for eqQ_X and the very precisely known value for $v'' = 0$, the errors estimated for this measurement are probably to small. Additionally, the values of eqQ derived in [37] for the different lines R(0) to R(10) and P(1) to P(5) of the same band vary by more than 10 MHz.

As already pointed out in Section 2, the quantum number dependences of the effective eqQ parameters are dominated by the dependence of eqQ on the nuclear distance R. A description of the dependences of $eq(R)Q_B$ and $eq(R)Q_X$ on R would allow for a determination of the R-dependence of the projection of the electrical field gradient $q(R)$, and one might expect to reach a satisfactory description of the functional form of eqQ with a reduced number of fit parameters, since both the v and the J-dependence are included in the R-dependence of eqQ. For this goal one has to discuss the adequate ansatz of the functional form of eqQ in relation to the molecular potentials. This is not within the scope of this work.

7 Prediction accuracy by interpolation

The formulae (10–15) permit a precise interpolation of the hyperfine parameters for rovibronic transitions in the visible to the near infrared spectral range. The (2σ) prediction uncertainties of the different parameters are estimated to be:

ΔeqQ: ±50 kHz, ΔC: ±2 kHz, $\Delta\delta$: ±3 kHz, Δd: ±4 kHz.

To give an overview of the variation of the uncertainties of the prediction formulae we choose the quadrupole coupling eqQ. Equations (14, 15) allow for a precise prediction of eqQ parameters in the range $v'' = 0$–17 for the ground state and $v' = 0$–43 for the B state. Due to the structure of the experimental data used for the fit the prediction accuracies for the eqQ parameters depend on the vibrational and rotational quantum numbers. Figure 6 shows the prediction accuracy for ΔeqQ for different vibrational bands and for the angular momenta $J' = 30$, 70 and 110. These specific bands are chosen, because they are the strongest vibrational bands in the visible spectral range and might be used for calibration purposes by other people. In general, for the considered range the largest uncertainties of the interpolated ΔeqQ values are observed for high J' and low v', and the uncertainties decrease with decreasing J' and increasing v'. The worst prediction uncertainty is still less than 50 kHz and on the average less than 20 kHz, which means about 10^{-5} relative accuracy.

The uncertainties of the calculated hyperfine splitting caused by the uncertainties of the different hyperfine parameters vary for different hyperfine components

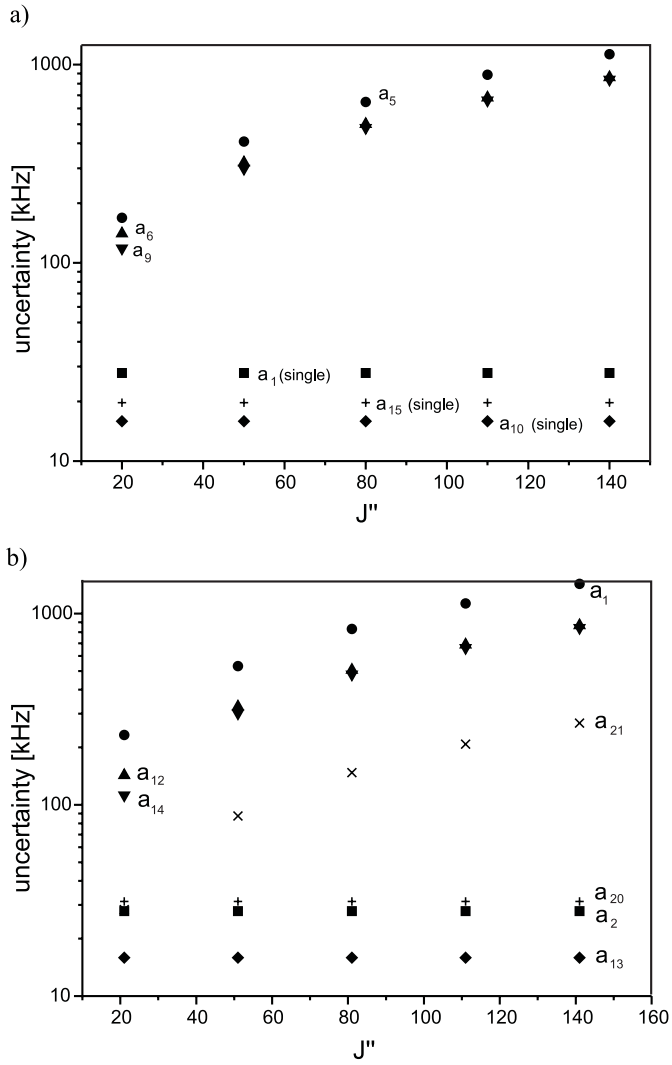

Fig. 7. Prediction uncertainties for selected hyperfine components of R(J'') lines of the 16–2 band. Panel (a): even J'', (b): odd J''. Each symbol specifies a selected hyperfine component.

of one rovibronic transition due to the geometrical factors $g_i, (i = eqQ, ...)$ of equation (2). Especially the influence of the spin-rotation parameter C increases with increasing angular momentum J. In order to test the prediction accuracy reached for the hyperfine structure, we investigated, how the hyperfine splittings for different hyperfine components vary, if the hyperfine parameters are changed within their prediction uncertainties stated above. These examinations were performed examplarily for the 16–2 vibrational band. The resulting uncertainties are shown in Figure 7 for different hyperfine components and as a function of J''.

For the hyperfine components $F - J = 0$ (components a_1, a_{10} and a_{15} for J'' even, and a_2, a_{13} and a_{20} for J'' odd) the uncertainty is nearly independent of J'' and relatively small ($\leq$30 kHz). For the other components the uncertainty is of the order of 100 kHz for low J'' and increases to nearly 1 MHz for $J'' = 140$. The reason for this is the uncertainty of the parameter C, whose influence is very small for $F - J = 0$ components. For the other components the influence of C increases nearly proportional to $\sqrt{J''}$. Therefore and due to their position in the hyperfine spectra the components a_1, a_{10}, a_{15} for J'' even and a_2, a_{13}, a_{20} for J'' odd are most suitable for use as frequency references. For transitions with even J'' these components are nonoverlapping lines, which are well separated from all other components (marked "single" in Fig. 7), and are located at the low (a_1) or high (a_{15}) frequency edge of the spectrum or roughly in the center (a_{10}). For odd J'' these components are in the middle of groups of three lines, so that the frequency pulling due to overlapping line profiles nearly cancels for these components. The lowest uncertainty (<20 kHz) is found for the central $F - J = 0$ component (a_{10} for even J'' and a_{13} for odd J''). Therefore, for the calculation of absolute transition frequencies of hyperfine components $F - J = 0$ the contribution to the relative uncertainty due to the interpolation of the hyperfine structure by the new formulae is about $3–5 \times 10^{-11}$, which is an improvement of nearly two orders of magnitude, as compared with interpolation formulae reported before.

8 Conclusion

Very precise interpolation formulae for the prediction of the $^{127}I_2$ molecule could be derived improving the prediction accuracy for the hyperfine splitting by nearly two orders of magnitude, as compared with the most accurate interpolation formulae published before. This was achieved for 3 different reasons:

1. extensive systematic measurements on the hyperfine structure in the NIR,
2. a systematic reanalysis of the literature data available, leading to a consistent data set for the iodine hyperfine parameters,
3. the functional forms of the interpolation formulae base on the physical origin of the different contributions.

For the first time rotational dependences of the ΔeqQ and ΔC parameters were systematically investigated for different vibrational bands. Both for $eqQ_X(v'', J'')$ and $eqQ_B(v', J')$ (for $v'' \leq 17$ and $v' \leq 43$) precise interpolation formulae were derived. The quantum number dependences of eqQ_B and eqQ_X are successfully described using expansions for powers of $(v + 1/2)$ and $J(J + 1)$. In contrast to the magnetic hyperfine parameters, where the quantum number dependence is nearly completely determined by the mixing with other electronic states, for the eqQ parameter and for the considered range ($v' \leq 43$, $v'' \leq 17$) this quantum number dependence is dominated by the R-dependence of the electrical field gradient $q(R)$ from the electron distribution.

The range of vibrational levels of the ground state is much bigger than for former investigations (*e.g.* [22,23]). Therefore, in contrast to the formulae as derived *e.g.* by

Razet *et al.* or by Arie *et al.* our new formulae have to include also the v'' and J'' dependence of eqQ_X. Due to the correlation between eqQ_X and eqQ_B for $eqQ_X(v'' > 0)$ this was not possible before. Using the precise measurements of $eqQ_X(v'' = 14,\ 15,\ J'' = 1)$ presented here we succeeded in separating the vibrational correlation between eqQ_B and eqQ_X. However, the correlation concerning the J-dependence of these parameters could not be broken so far. This could perhaps be reached analysing the R-dependence of the eqQ parameters.

Former interpolation formulae presented for ΔeqQ *e.g.* by Razet *et al.*, by Arie *et al.* and by Morinaga are not suitable for the description of the eqQ parameters in the NIR spectral range, because these transitions start from fairly high excited vibrational levels in the ground state and their formulae cannot describe the variation of eqQ_B and eqQ_X simultaneously. Furthermore, in the formulae by Arie *et al.* no rotational dependence of the eqQ parameter is considered.

For the first time for low vibrational levels $v'' \leq 17$ a vibrational dependence of C_X was observed and described by a simple interpolation formula. The variation is necessary mainly to explain the precise data obtained in the NIR, but it is also significant for an improvement of the interpolation formulae for ΔC, because the total variation of $C_X(v'')$ for $0 \leq v'' \leq 17$ is a little bit larger than 1 kHz, which is the prediction uncertainty of C_B, where an improved interpolation formula was found for $(v' \leq 43,\ J')$. The restriction in v' was set, because for $v' > 43$ the increasing perturbations due to other electronic states would have demanded for a much more complicated formula, and the data amount in the literature is not sufficient for a high precision description.

For the nuclear spin-spin interaction no rotational dependence was observable, but precise interpolation formulae for the vibrational dependence could be determined. For the parameters δ_B and d_B the local perturbation in the range $v' \leq 17$ due to the crossing 1_u state could be identified and was accounted for in the interpolation formulae. This crossing also produces the predissociation of the B state in iodine.

With these results a complete set of interpolation formulae for all significant hyperfine parameters for the range $v' \leq 43$, $v'' \leq 17$ and $J'' \leq 200$ is available. The use of these formulae allows to calculate the hyperfine splitting for the $F - J = 0$ components with an uncertainty of 20–30 kHz. For other hyperfine components the prediction accuracy increases nearly linearly with $\sqrt{J''}$ from 100 kHz for $J'' = 0$ to 1 MHz for $J'' = 150$.

For the calculation of recommended transition frequencies with hyperfine components $F - J = 0$ the relative uncertainty contribution due to the interpolation of the hyperfine structure is less than 5×10^{-11}, but the achievable absolute accuracy depends on that of the pure rovibronic transition frequency. We will report on the prediction of such frequencies applying precise potential curves in a forthcoming paper [43]. An interactively usable electronic iodine atlas is already available as software package [44], applying these new interpolation formulae and the precise potential functions.

This work was supported by Deutsche Forschungsgemeinschaft. Discussions with Chr. Bordé, who also showed us his results prior to publication, are gratefully acknowledged.

References

1. T.J. Quinn, Metrologia **36**, 211 (1999).
2. C.J. Bordé, G. Camy, B. Decomps, J.-P. Descoubes, J. Vigué, J. Phys. France **42**, 1393 (1981).
   C.J. Bordé, G. Camy, B. Decomps, Phys. Rev. A **20**, 254 (1979).
3. F.-L. Hong, J. Ishikawa, Opt. Commun. **183**, 101 (2000).
4. F.-L. Hong, J. Ye, L.-S. Ma, S. Picard, C.J. Bordé, J.L. Hall, J. Opt. Soc. Am. B **18**, 379 (2001).
5. J. Ye, L. Robertsson, S. Picard, L.-S. Ma, J.L. Hall, IEEE Trans. Instrum. Meas. **48**, 544 (1999).
6. M.L. Eickhoff, J.L. Hall, IEEE Trans. Instrum. Meas. **44**, 155 (1995).
7. C.S. Edwards, G.P. Barwood, P. Gill, F. Rodriguez-Llorente, W.R.C. Rowley, Opt. Commun. **132**, 94 (1996).
8. S. Kremser, B. Bodermann, H. Knöckel, E. Tiemann, Opt. Commun. **110**, 708 (1994).
9. C.S. Edwards, G.P. Barwood, P. Gill, W.R.C. Rowley, Metrologia **36**, 41 (1999).
10. A. Razet, J. Gagnière, P. Juncar, Metrologia **30**, 61 (1993).
11. H.R. Simonsen, IEEE Trans. Instrum. Meas. **IM46**, 141 (1997).
12. S. Gerstenkorn, P. Luc, *Atlas du spectre d'absorption de la molécule d'iode*, Laboratoire Aimé Cotton, CNRS II, 91405 Orsay (France), 14 000 cm^{-1}–15 600 cm^{-1} (1978), 15 600 cm^{-1}–17 600 cm^{-1} (1977), 17 500 cm^{-1}–20 000 cm^{-1} (1977); S. Gerstenkorn, J. Vergès, J. Chevillard, *Atlas du spectre d'absorption de la molécule d'iode*, Laboratoire Aimé Cotton, CNRS II, 91405 Orsay (France), 11 000 cm^{-1}–14 000 cm^{-1} (1982).
13. S. Gerstenkorn, P. Luc, J. Phys. France **46**, 867 (1985).
14. I. Velchev, R. van Dierendonck, W. Hogervorst, W. Ubachs, J. Mol. Spectrosc. **187**, 21 (1998).
15. S.C. Xu, R. van Dierendonck, W. Hogervorst, W. Ubachs, J. Mol. Spectrosc. **201**, 256 (2000).
16. M. Broyer, J. Vigué, J.C. Lehmann, J. Phys. France **39**, 591 (1978).
17. J. Vigué, M. Broyer, J.C. Lehmann, Phys. Rev. Lett. **42**, 883 (1979).
18. J.P. Pique, F. Hartmann, S. Churassy, R. Bacis, J. Phys. France **47**, 1909 (1986) (part I), 1917 (part II).
19. M. Gläser, PTB-Bericht, PTP-Opt-25 (1987).
20. V. Spirko, J. Blabla, J. Mol. Spectrosc. **129**, 59 (1988).
21. A. Morinaga, K. Sugiyama, N. Ito, J. Helmcke, J. Opt. Soc. Am. B **6**, 1656 (1989).
22. A. Arie, R.L. Byer, Opt. Commun. **111**, 253 (1994).
23. A. Razet, S. Picard, Metrologia **33**, 19 (1996), and references therein.
24. A. Razet, S. Picard, Metrologia **34**, 181 (1997), and references therein.
25. A. Yokozeki, J.S. Muenter, J. Chem. Phys. **72**, 3796 (1980).

26. J.-P. Wallerand, F. duBurck, B. Mercier, A.N. Goncharov, M. Himbert, Ch.J. Bordé, Eur. Phys. J. D **6**, 63 (1999).
27. H. Knöckel, S. Kremser, B. Bodermann, E. Tiemann, Z. Phys. D **37**, 43 (1996).
28. P. Gill, J.A. Clancy, J. Phys. E: Sci Instrum. **21**, 213 (1988).
29. S. Churassy, G. Grenet, M.L. Gaillard, R. Bacis, Opt. Commun. **30**, 41 (1997).
30. J.B. Koffend, S. Goldstein, R. Bacis, R.W. Field, S. Ezekiel, Phys. Rev. Lett. **41**, 1040 (1978).
31. H. Belaidi, M. Himbert, Y. Millerioux, A. Razet, P. Juncar, IEEE Trans. Instr. Meas. **44**, 461 (1995).
32. R.P. Hackel, S. Ezekiel, Phys. Rev. Lett. **42**, 1736 (1979).
33. J.B. Koffend, Ph.D. thesis, M.I.T., Cambridge, Mass, 1978.
34. R.P. Hackel, K.H. Castleton, S.G. Kugolich, S. Ezekiel, Phys. Rev. Lett. **35**, 568 (1975).
35. J.P. Pique, F. Hartmann, R. Bacis, S. Churassy, Opt. Commun. **36**, 354 (1981).
36. R. Bacis, M. Broyer, S. Churassy, J. Vergès, J. Vigué, J. Chem. Phys. **73**, 2641 (1980).
37. M. Wakasugi, T. Horiguchi, M. Koizumi, Y. Yoshizawa, J. Opt. Soc. Am. B **5**, 2298 (1988).
38. J. Vigué, M. Broyer, J.C. Lehmann, J. Phys. France **42**, 937 (1981) (parts I–III).
39. E. Martínez, M.T. Martínez, F. Castano, J. Mol. Spectrosc. **128**, 554 (1988).
40. F. Bertinetto, P. Cordiale, S. Fontana, G.B. Picotto, IEEE Trans. Instr. Meas. **IM-36**, 609 (1987).
41. W.-Y. Cheng, J.-T. Shy, T. Lin, Opt. Commun. **156**, 170 (1998).
42. C.J. Bordé, private communication, 2001.
43. H. Knöckel, B. Bodermann, E. Tiemann, to be published.
44. See `www.toptica.com`.